S.S. () ELSEVIER

Contents lists available at ScienceDirect

Materials and Design

journal homepage: www.elsevier.com/locate/matdes



Effect of indium accumulation on the growth and properties of ultrathin In(Ga)N/GaN quantum wells



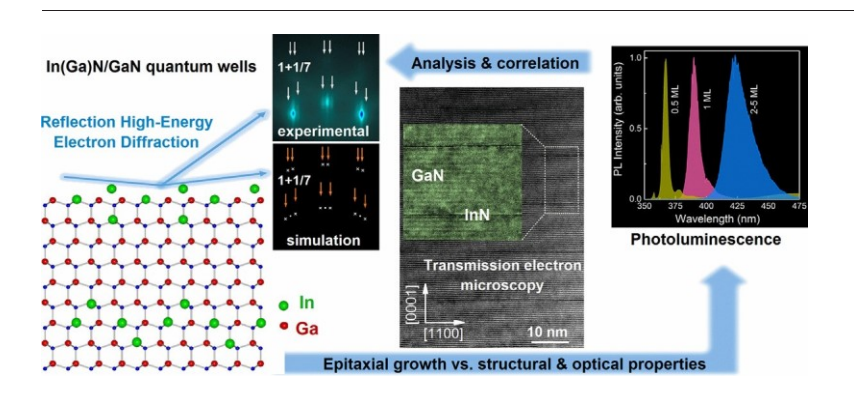
Chen Li^a, Yurii Maidaniuk^a, Andrian V. Kuchuk^a,*, Yuriy I. Mazur^a,*, Mourad Benamara^a, Morgan E. Ware^{a,b}, Gregory J. Salamo^a

- ^a Institute for Nanoscience and Engineering, University of Arkansas, Fayetteville, AR 72701, USA
- ^b Department of Electrical Engineering, University of Arkansas, Fayetteville, AR 72701, USA

HIGHLIGHTS

- High temperature (N 500 oC) growth of ultrathin InN/GaN quantum wells (QWs) demonstrates a self-limiting process resulting in monolayer thicknesses.
- The InN deposited after the saturation point decomposes at the high growth temperatures resulting in surface indium accumulation during the growth.
- An incommensurate layer of indium with a characteristic reflection highenergy diffraction pattern develops during the growth of InN/GaN QWs.

GRAPHICAL ABSTRACT



article info

Article history:
Received 18 November 2019
Received in revised form 8 February 2020
Accepted 11 February 2020
Available online 12 February 2020

Keywords:
InN
MQW
PAMBE
RHEED
Epitaxy
Growth model

abstract

In this work, we present the investigation of InN/GaN multiple-quantum-well (MQW) growth by plasma-assisted molecular beam epitaxy using in-situ reflection high-energy electron diffraction (RHEED) to monitor the growth process. The analysis of the RHEED intensity and pattern transitions identified an indium surface accumulation even with a nominal thickness of InN as small as 0.5 monolayer (ML). This result explicitly shows that, even at low growth temperatures of ~ 550 °C, not all of the supplied indium is incorporated into the quantum well (QW). Moreover, the residual indium can become incorporated into the GaN matrix on either side of the QW. Both QW thickness and the photoluminescence (PL) emission energy showed a self-regulating behavior. The apparent thickness did not exceed 2 MLs even when the deposited InN thickness is as large as 5 MLs. The PL emission shows a continuous redshift with the deposited InN from ~ 370 nm for 0.5 ML until it saturates at ~ 423 nm for N2 ML. Based on the observed growth phenomena, a qualitative growth model was developed to explain the self-limited epitaxial growth of ultrathin In(Ga)N/GaN QWs.

© 2020 The Authors. Published by Elsevier Ltd. This is an open access article under the CC BY license (http://creativecommons.org/licenses/by/4.0/).

1. Introduction

Since InGaN films demonstrated band edge emission in 1992 [1], InGaN-based blue light emitting diodes (LEDs) [2] and lasers [3] have achieved great commercial success. However, given that the direct band gap covers the spectral range from ultraviolet (GaN 3.4 eV) to

^{*} Corresponding authors.

E-mail addresses: kuchuk@uark.edu (A.V. Kuchuk), ymazur@uark.edu (Y.I. Mazur).

infrared (InN 0.6 eV), the full potential of InGaN is far from fully realized. The challenge has been in the growth of high quality InGaN films with high indium (In) content. However, due to the significant differences in physical properties between GaN and InN, many challenges in epitaxial growth remain. In addition to possible defects generation caused by lattice mismatch, alloying phenomena such as phase separation, composition pulling, and chemical ordering may also contribute to the deterioration of film quality [4,5]. Further, owning to the weak InNN bonds, the common InGaN growth temperature is not high enough to ensure the growth of high quality GaN and AlGaN layers, which are often used to sandwich the InGaN active layers to form quantum wells (QWs) in real devices. As a result, there are only a limited range of QW compositions available and therefore a limited range of spectral emission obtainable.

In order to address this problem, Yoshikawa et al. explored the possibility of growing InN/GaN QWs [6,7] using molecular beam epitaxy (MBE) at a temperature range much higher (N~650 °C) than the InN dissociation temperature of ~500 °C. In this temperature range, it turns out that the thickness of the QWs is self-limited to 1 to 2 monolayers (MLs) with atomically abrupt interfaces. This, however, is encouraging, because the 1 or 2 ML QW of InN can subsequently be used as building blocks to grow multiple quantum wells (MQWs) or super lattices (SLs) of InN/(Al)GaN with effective optical emission close to that of pure InN. This alternative to the growth of thick InGaN appears to avoid many of the potential alloying problems and should achieve better QW material quality due to higher growth temperatures (over 650 °C).

Interestingly, the structural property as well as the growth mechanism of InN/GaN QWs using ultra-thin, 1 to 2 MLs, InN, is still under debate. One reason is that the reported photoluminescence (PL) data show large variations, with emission found anywhere from 2.8 eV to 3.3 eV [6-15]. Yoshikawa et al. found that, at relatively low growth temperatures, the QW thickness can be controlled between 1 or 2 MLs with a resulting PL emission peak varying between ~390 nm and ~430 nm [16,17]; while at high growth temperatures only 1-ML- or a fractional-ML thick QW can be formed. However, a more recent study by Wolny et al. [18], using growth temperatures between 480 °C and 650 °C could not confirm the existence of 2-ML-thick QWs. Another reason for the debate is that first principle calculations [19-21] predict that the emission band of an ideal GaN/1-ML-InN/GaN QW is b2.2 eV, which is significantly lower than all PL observations. This indicates a possible resolution by which the nominal InN QWs are altered by intermixing with Ga resulting in an InGaN alloy. By analyzing lattice expansion in the vicinity of the QWs using transmission electron microscopy (TEM), Suski et al. [22] concluded that the actual indium content for a nominal 1-ML-thick InN quantum well is around 33%. This was later confirmed and strengthened by G. P. Dimitrakopulos et al. [23], again by TEM. Despite the possible indium enrichment in neighboring layers, the indium content in the central layers is estimated to be ~0.23 and ~0.33 respectively for 1-ML- and 2-ML-thick QWs. Similar indium concentrations for 1-ML QWs were also obtained in Ref. 18. More-

more recently to a 2 3 2 3 Re00° surface reconst ruction [24], quickly appears when depositing the nominal InN QWs, it had been proposed that the 1-ML-thick QW is in-fact just the preserved surface reconstruction [15]. This argument is supported by the 3× indium atom ordering observed by TEM [24]. Thus, the discrepancy between the data described above indicates that the actual structure and composition of the InN QWs may be specific to the detailed growth conditions.

In the present work, we focus on studying the growth process of InN/ GaN MQWs at a growth temperature of 550 °C using plasma-assistant molecular beam epitaxy (PAMBE). This temperature is relatively low to achieve high quality GaN films, but is far above the decomposition temperature of InN thin films. However, this turns out to be an interesting medium temperature where the desorption of In metal is negligible.

In that way, we can study controversial debated topics, such as: (i) the intermixing between Ga adatoms and the InN QW, (ii) the In accumulation during the growth as a result of an exchange between the In atoms of the QW and the Ga adatoms and (iii) the effect of In accumulation on the growth and properties of ultrathin In(Ga)N/GaN QWs.

2. Growth of InN/GaN MQWs

The sample growths were performed on iron-doped, semi-insulating, hydride vapor phase epitaxy (HVPE)-grown on sapphire, GaN templates (Kyma) in a VEECO Gen II MBE system equipped with a RHEED system. The fluxes of the group III species were provided by thermal effusion cells, and a VEECO UNI-Bulb radio frequency (RF) plasma source was used to generate active nitrogen flux. For all growths, the RF power was fixed at 350 W and the nitrogen flow was fixed at 0.5 sccm, which leads to a nitrogen limited low temperature GaN growth rate of 0.26 ML/s.

The growth procedure is expressed by the shutter sequence shown in Fig. 1(a) and the sample structure is shown schematically in Fig. 1 (b). The nitrogen shutter was kept open throughout the growth, and the nominal InN quantum well thickness was controlled by the combination of indium flux and open shutter time. A GaN buffer was grown at ~790 °C under slight gallium-rich (Ga-rich) conditions prior to each MQW to ensure a good surface morphology. After the buffer growth and thermal desorption of surface gallium droplets, samples were cooled to 550 °C for n-ML-InN/GaN MQWs growth. Here, n denotes the nominal thickness in monolayers of the InN layer, while the GaN spacer layers were 15 nm thick to avoid strain build up due to successive In N QWs. For n = 1, 3, and 5, the indium flux was 0.26 ML/s, while the open shutter times were 4 s, 12 s, and 20 s, respectively. For n = 0.5, the open shutter time and the indium flux were 4 s and 0.13 ML/s, respectively. A growth interruption (GI) of 2 s was inserted before each GaN spacer layer to ensure the indium shutter was fully closed before the opening of the gallium shutter. A slightly Ga-rich growth condition was used during the growth of the GaN spacer not only for good morphology and crystal quality, but also to prevent indium from being incorporated into the GaN spacers [11,25]. After closing the gallium shutter, another GI (75–100 s) was inserted to let the active nitrogen flux consume any excess gallium that might have accumulated on the surface.

3. RHEED intensity analysis

MQWs consisting of 10 repeats of the InN/GaN bilayer with nominal InN thicknesses of 0.5, 1, and 3 MLs were used to study the RHEED intensity variations during growth. These MQWs were grown subsequently on the same substrate without removal from the growth chamber to ensure comparability. Between subsequent MQW stacks, a high temperature (~790 °C) GaN buffer was grown to recover a pristine surface morphology.

The specular reflection in the RHEED intensity pattern was monitored along the \$1120 azimuthal direction. Throughout the entire

study, the monitored RHEED pattern remained streaky, indicating that the growth progressed under metal-rich condition as planned. The RHEED intensity evolution during the 1-ML-InN/GaN MQW growth is shown in Fig. 2(a). To further reveal fine features, the magnified view of the second InN/GaN growth cycle (shaded area in Fig. 2(a)) is shown as Fig. 2(b).

As is seen in Fig. 2(b), immediately after the opening of indium shutter, the RHEED intensity shows a noticeable spike first, and then a fast decay follows until the indium shutter was closed. The initial intensity spike has been shown to be caused by metal adatoms with higher electron density covering the physically adsorbed nitrogen atoms [26]. Since InN growth is prohibited at this growth temperature and the indium desorption is negligibly small, the subsequent rapid intensity

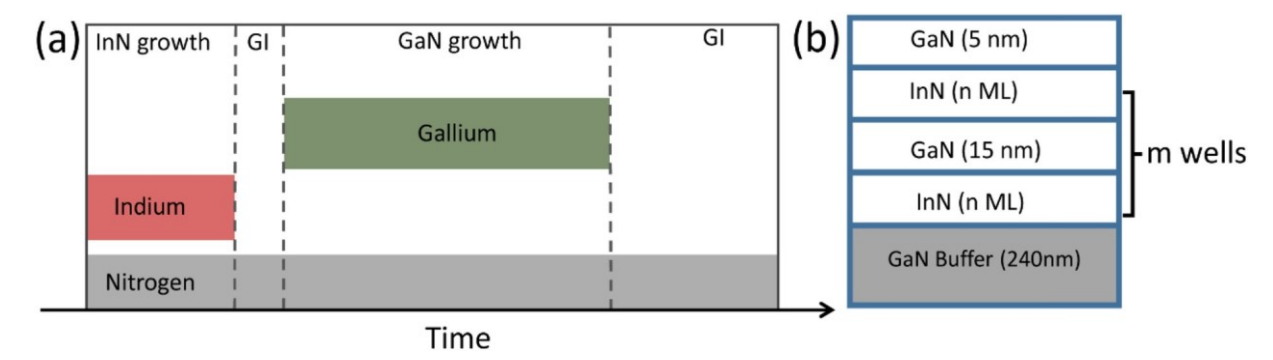


Fig. 1. (a) Shutter sequence for one InN/GaN bilayer growth cycle; (b) Sample structure.

decay is due to the buildup of a liquid-like indium adlayer, which continues until the indium shutter is closed.

After the short GI of 2 s, the RHEED intensity increases sharply to a relatively high maximum following the Ga shutter opening, then almost as quickly decays to a stable level until the gallium shutter is closed. This behavior is similar to the observation in our previous study [27] of high temperature InN/GaN MQW growth. The intensity increase here is mainly attributed to the stronger electron scattering of gallium species compared to that of indium. Afterwards, as the growth continues, the gallium overpressure eventually leads to a liquid-like adlayer and droplet accumulation on surface. As a result, the RHEED intensity starts to decay.

After gallium accumulation reaches a critical amount, the intensity stops declining and stays at a saturated level. This saturated level, referred as "level A" hereafter, is the result of the surface being covered with excessive gallium droplets and is nearly a constant in all growth cycles (indicated by the gray dotted lines in Fig. 2).

Following the GaN spacer growth, during the second GI, the RHEED intensity eventually recovers to a new stable level, which is traced by the red dotted lines in Fig. 2. This is "level B," which can be seen to decay over the course of the successive QW growths. The recovery during this GI period, however, consists of two distinct stages. During the first stage, the RHEED intensity changes only slightly while the excess Ga is consumed by the active nitrogen to form additional GaN. Below some critical level of gallium coverage, the recovery enters the second stage characterized by a fast intensity increase, where the final excess Ga is consumed leaving a Ga-free GaN surface at a new stable RHEED

intensity, level B, indicated by red dotted lines in Fig. 2. It is worth mentioning that, contrary to level A that changes very little throughout the growth, level B shows a dependence on subsequent growth cycles. Infact, as is shown by the red dotted line in Fig. 2(a), level B is initially more intense than level A, but within a few cycles, it has decayed such that it is below level A. This dropping of level B can be explained by indium accumulation. During InGaN bulk growth, it is well known that the determining factor for indium incorporation is the Ga/N flux ratio. Because of the preferential incorporation of gallium, indium would only incorporate when Ga/N flux ratio is smaller than unity [28,29]. Therefore, if only a portion of the deposited 1-ML indium can be incorporated into the nominal single monolayer quantum well, the residual indium would float on the growth front, propagate vertically during GaN growth and increase its volume every time after a new nominal InN QW growth. This scenario would explain why level B continuously decreases towards a low saturated level.

Two more MQWs with larger (n = 3) and smaller (n = 0.5) nominal InN thickness were grown for RHEED intensity study and the results are shown in Fig. 3. Although different in shape and magnitude, all features discussed for n = 1 in Fig. 2 can be found for n = 3 and n = 0.5. For n = 3, the indium deposition is so large that it only takes 3 cycles to saturate level B, and, after the third cycle, the level B becomes invariant through each subsequent cycle. It is worth mentioning that the saturated level B is lower than that of level A, which supports the arguments that gallium adsorption was mainly responsible for the RHEED intensity increase in the beginning of GaN spacer growth. In sharp contrast, for the case of n = 0.5, level B decreases so slowly that the RHEED intensity

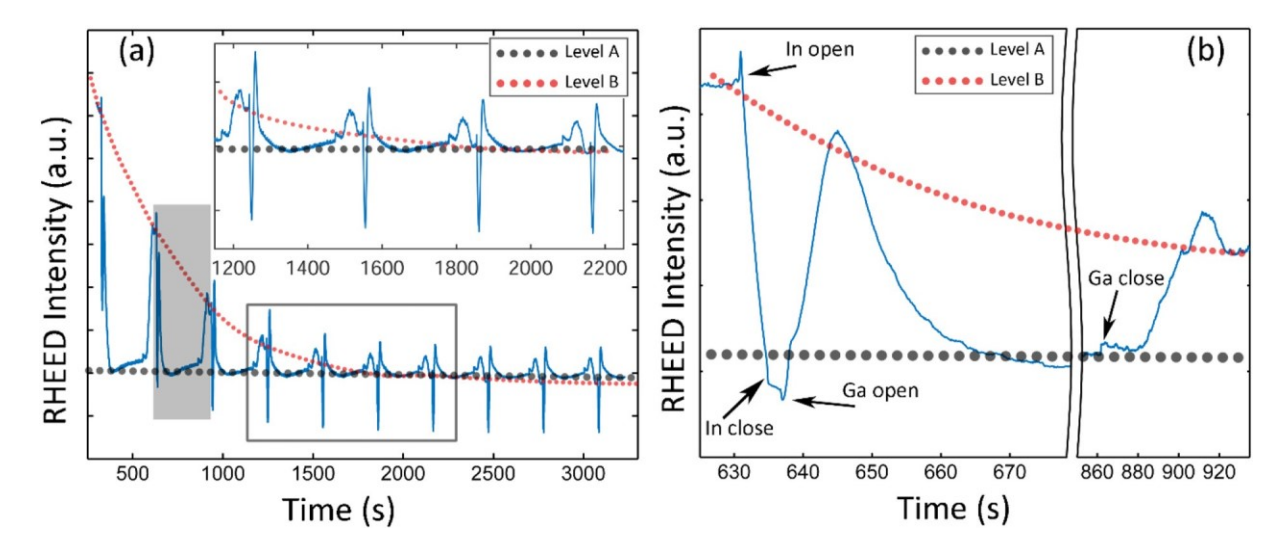


Fig. 2. (a) RHEED intensity evolution of 1-ML-InN/GaN MQW growth. The inset is a magnified view of the hollow rectangular area; (b) Zoomed view of the RHEED intensity evolution of one InN/GaN bilayer growth cycle (shaded area in (a)). The gray and red dotted lines in (a) and (b) are only guides showing the general evolution of levels A and B, respectively. Levels A and B are associated with the surface being covered with excessive gallium and indium adatoms, respectively.

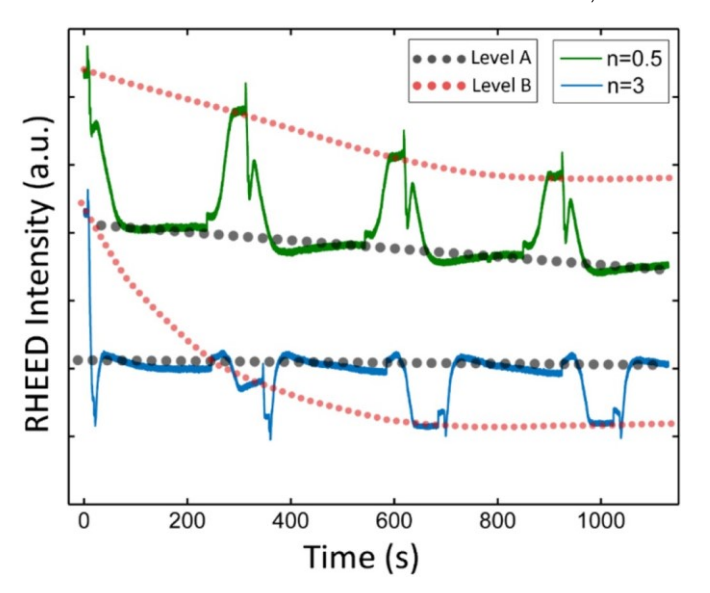


Fig. 3. RHEED intensity evolution of n-ML-InN/GaN MQWs growth (first 4 cycles) for n = 0.5 and n=3. The gray and red dotted lines are eye-guides for the evolution of level A and level B, respectively.

fluctuations appear to be similar for all growth cycles. Nonetheless, the accumulation of indium is still recognizable by observing the RHEED pattern transitions in the following discussions.

4. RHEED pattern analysis

More details of the MQW growth were revealed by analysis of the RHEED pattern transitions. After the high temperature buffer growth and desorption of gallium droplets, the surface showed a GaN 1×1 reconstruction (see Fig. 5(a)). Prior to growth, cooling the GaN surface to

550 °C lead to a faint 2 × 2 RHEED pattern, which was likely caused by nitrogen adsorption [24]. Side experiments showed that, at 550 °C, when a bare GaN surface is covered with ~1/3 ML of indium under active nitrogen irradiation, a faint "1×3" pattern is discernible. In our system, the " 1×3 " pattern became well defined when the temperature was higher than ~590 °C. The RHEED patterns viewed along the 1120 azimuth when level B is reached in different InN/GaN growth cycles for different nominal InN thicknesses are shown in Fig. 4. For the growth with nominal InN thickness of 1 ML, the "1×" pattern remained through the first cycle and the majority of the second cycle, even though the intensity fluctuated. However, when level B was reached during the second cycle, a new pattern appeared. This pattern was characterized by sidebands appearing around the "1x" streaks (labeled by white arrows in Fig. 4). Although becoming dimmer, this pattern also survived the InN deposition stage of the third growth cycle. However, once the gallium shutter was opened, it quickly changed back into the "1×" pattern and only reappeared when the intensity went back to level B again. This alternating appearance of the "1×" pattern and the new pattern were observed in all subsequent growth cycles. However, each time the new pattern appeared it was dimmer than before. This corresponded to the dampening of level B by indium accumulation in Figs. 2 and 3. The RHEED pattern transforms in a similar manner for n = 3 and n = 0.5. For n = 3, the "1×" pattern changed into the new pattern during the first InN/GaN growth cycle; while, for n = 0.5, the new pattern only became well defined following the sixth cycle.

As is shown in Fig. 4, the distance between sidebands to the nearest "1×" streaks is best to be estimated as 1/7 of the "1×" streak spacing. This will be referred as "1 + 1/7" hereafter to follow the convention used in the work by Smith et al. [30], in which a similar RHEED pattern had been observed on a Ga-rich GaN(0001) surface below 350 °C. This surface was explained to be caused by multiple scattering of the electron beam between a GaN 1 × 1 surface and an incommensurate overlayer [30–32].

Further experiments were performed in order to identify the origin of the 1 + 1/7 pattern. It was found that the pattern can be reproduced

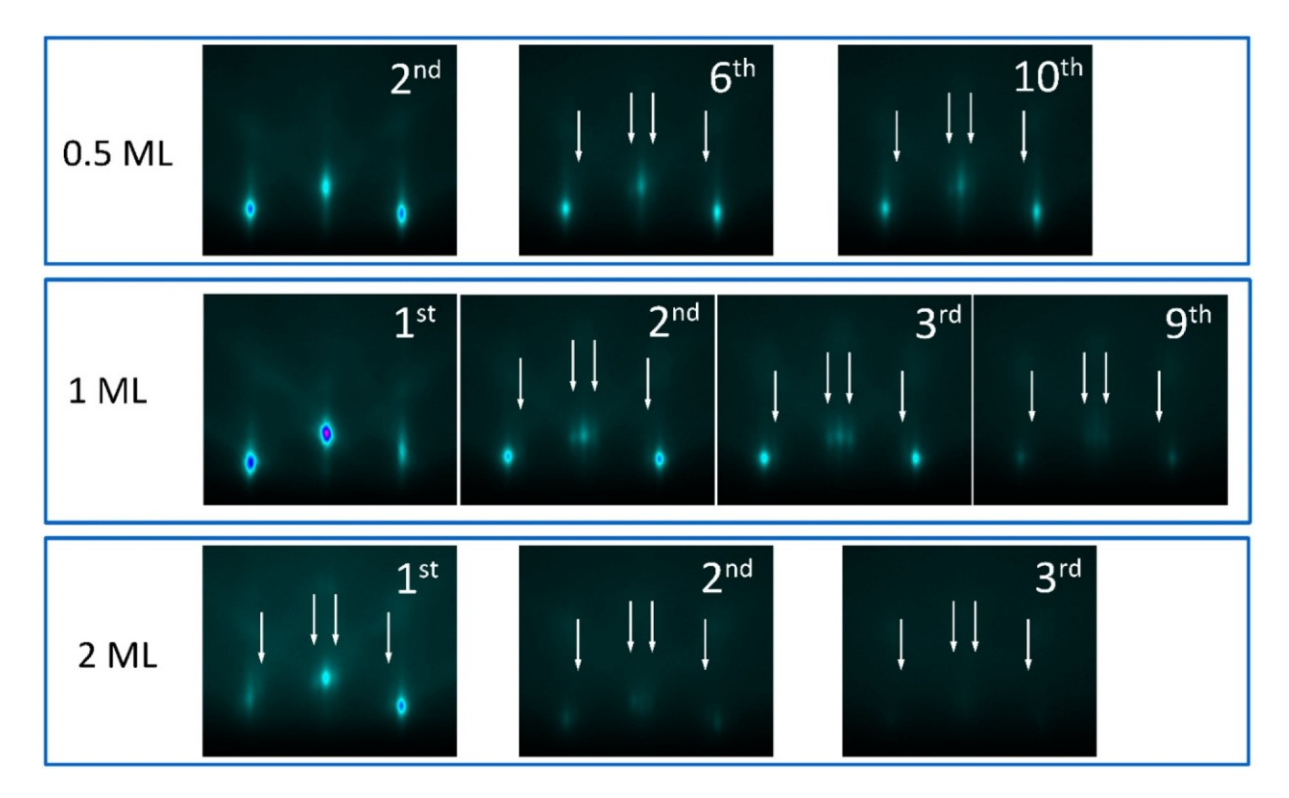


Fig. 4. RHEED patterns viewed along \$1120] azimuth during different InN/GaN growth cycles when level B is reached. The positions of side streaks are labeled by white arrows. The top, middle, and bottom row correspond to nominal InN thickness of 0.5, 1, and 2 MLs.

consistently at 550 °C following the InN/GaN growth sequence shown in Fig. 1(a), i.e. deposit InN first, then grow GaN, and finally let active nitrogen to consume excess gallium. However, depositing either indium or gallium on the GaN(0001) surface, with or without active nitrogen irradiation, failed to produce this pattern. Further, at 550 °C, the "1 + 1/7" pattern is only stable under nitrogen flux irradiation, i.e., it persists for a relatively long time if the nitrogen shutter is open while quickly disappears once the nitrogen shutter is closed. Also, once the pattern has vanished, re-exposing the surface to active nitrogen does not restore it. However, the stability of the 1 + 1/7 pattern can be improved at lower growth temperatures. For instance, at 520 °C, the 1 + 1/7 pattern can last for a long time even without active nitrogen irradiation, and is, in general, better defined than patterns obtained at 550 °C.

Typical images of the 1 + 1/7 pattern obtained at 520 °C viewed along 1120] and 1100] are shown in Fig. 5(b) and (e), respectively, where white arrows label identifiable peaks/streaks other than those belonging to the 1×1 pattern. Since the behavior of the 1 + 1/7 pattern suggests that it is related to surface indium accumulation, a simulation is performed assuming an incommensurate overlayer sitting on a GaN 1 × 1 surface with the same in-plane symmetry as GaN but with a lattice constant is 7 ^{6}a (a is the in-plane lattice constant of GaN). This was programmed with MATLAB (version R2018b), taking into consideration direct scattering and double scattering corresponding to reciprocal space lattice vectors with small magnitude [31,32]. The resulting calculated intensity maxima are shown Fig. 5(c) and(f) and demonstrate a near perfect correlation with the measured RHEED patterns when using an electron energy of 16 keV (experimental setup) and incident angles of 4.5° and 4.3° for electron beams incident along $11\overline{2}$ and $1\overline{1}$ 00, respectively

Although never observed with RHEED in a MBE system, a similar surface reconstruction, induced by an incommensurate indium adlayer, was reported by C. Friedrich et al. [33] in an ex-situ annealing study of fully strained InGaN films using low energy electron diffraction (LEED) to characterize the surface. Therefore, taking into account the RHEED pattern simulation as well as results of the RHEED intensity analysis, we can confirm that the "1 + 1/7" pattern is produced by indium adlayers sitting on an InGaN layer.

Although the Ga-rich growth condition is used to prevent indium incorporation during the GaN spacer growth, the formation of InGaN layers is still possible when excess gallium is about to be fully consumed [16,25], presumably b1 ML. Consequently, the next InN QW growth could start on an InGaN surface with indium adlayers. A common practice to prevent the InGaN formation is to divide the second GI in Fig. 1 (a) into two steps [11,16,34]. During the first step the nitrogen shutter is closed and the indium accumulation on surface is thermally desorbed first due to the higher vapor pressure; then the nitrogen shutter is opened during the second step to consume residual gallium. This division was not adopted in this work because the indium desorption time is impractically large at 550 °C.

5. Structural and optical characterizations

The successful insertion of InN QWs and indium accumulation were revealed by ω-2θ X-ray diffraction (XRD) scans around the GaN(0002) reflection. The XRD measurements were performed using Philips X'pert MRD system. The diffractometer was equipped with a standard fourbounce Ge(220) monochromator, 1.6 kW Cu Kα1 X-ray tube and a Pixel detector. The results from the MQW samples with total QW number, m = 7, are shown in Fig. 6(a). Besides the two major peaks at ~17.29° and ~18.00° caused by bulk GaN(0002) and AlN(0002) seeding layers, the well-defined interference fringes are clearly seen for all samples with nominal indium thicknesses of 0.5, 1, 2, and 3 MLs. Furthermore, for the sample with n = 2, a bulk indium peak [35] can be observed at ~16.47° indicating indium droplet accumulation, and this peak becomes more pronounced for the sample with the largest nominal thickness (n = 3). This observation is in agreement with the faster saturation of level B (Figs. 2 and 3), as well as the faster dimming of the 1 + 1/7 RHEED pattern (Fig. 4) with larger nominal InN thicknesses.

The formation of QWs was further confirmed by cross-sectional TEM measurements. As it is shown in Fig. 6(b) and (c), the continuous QWs are found to be separated by ~ 14 nm GaN spacer layers. For both samples with the nominal QW thicknesses of 1 ML and 3 MLs, the QW thickness is no N2 MLs.

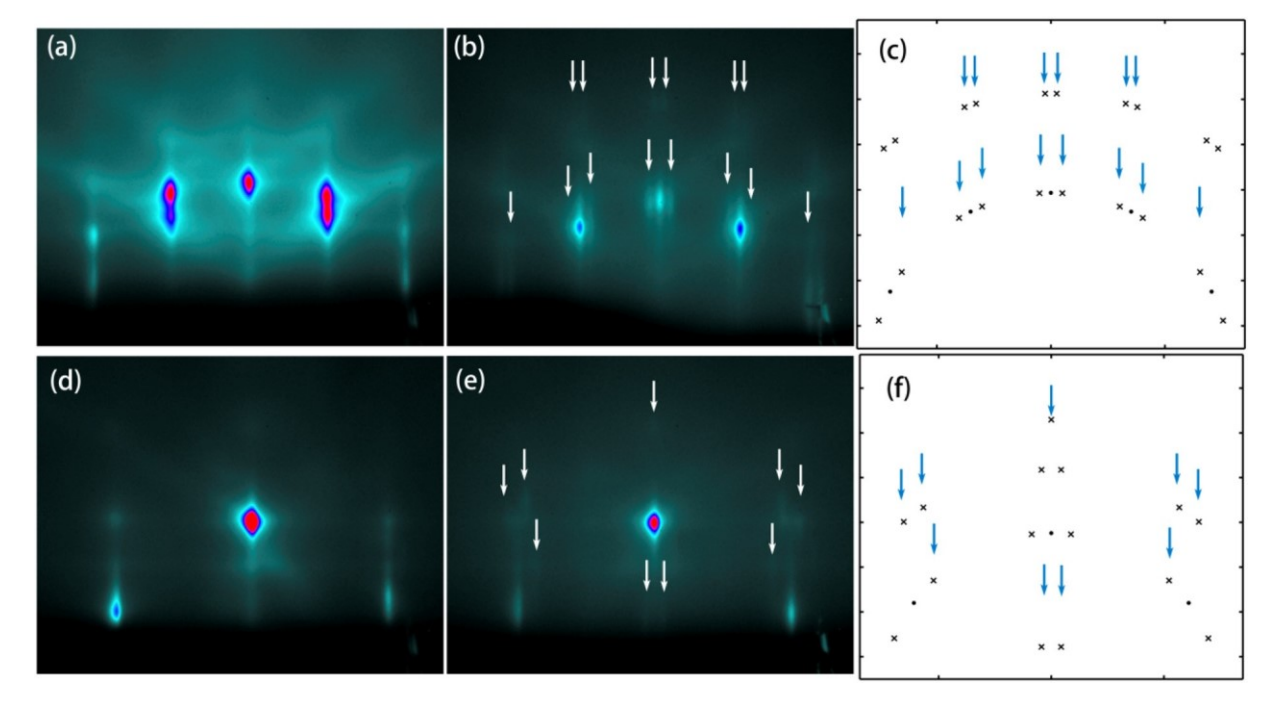


Fig. 5. (a) and (d) GaN 1×1 RHEED pattern viewed along \$1120] and \$1100] azimuth after high temperature GaN buffer growth; (b) and (e) The 1 + 1/7 RHEED pattern obtained at 520 °C viewed along \$1120] and \$1100] azimuth with identifiable streaks not belonging to the 1×1 pattern labeled by white arrows; (c) and (f) Simulated electron beam maxima caused by GaN 1×1 surface (dots), and by double scattering. The blue arrows in (c) and (f) correspond to the white arrows in (b) and (e).

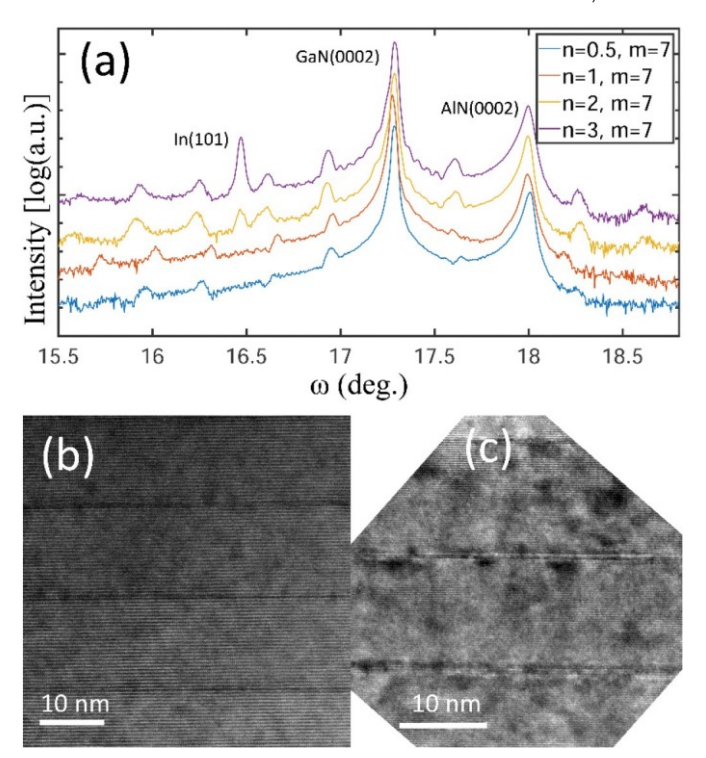


Fig. 6. (a) ω -20 XRD scans around the GaN(0002) reflection of samples grown at 550 °C with nominal thickness of n-ML InN and total QW number m = 7; (b) and (c) are high resolution bright field cross-sectional TEM images of MQWs with nominal InN thickness of 1 ML and 3 MLs, respectively.

Fig. 7 summarizes photoluminescence (PL) results of various samples with different number of QWs (m) and nominal QW thickness (n-ML). The PL was measured at a temperature of 10 K using the 532 nm line of a frequency doubled Nd:YAG laser, which was further doubled by a Coherent MBD 266 module to reach an excitation wavelength of 266 nm (4.66 eV). The PL signal from the sample was dispersed by a 0.32 m monochromator and detected by a liquid nitrogen cooled Si photodiode detector array. As is seen in Fig. 7(a), a clear trend is that changing the nominal thickness changes the emission energy up to a limit. The wavelength maximum of ~423 nm is reached when the nominal thickness is equal to or larger than 2-ML. This PL wavelength is nearly identical to what was reported by Yoshikawa et al. [16,17], which was confirmed to be from QWs with a 2-ML apparent thickness. Moreover, when the nominal thickness is 1-ML, the emission peaks lie in the range from 390 to 400 nm, which agrees well with

the PL emission from 1-ML thick QWs observed by various research groups [12,15–17,36]. For the smallest nominal thickness of 0.5-ML, the PL spectra shows a large variation over the sample surface, typically consisting of a weak main emission peak located between 360 nm and 380 nm and possible side peaks (see Fig. 7(b)). In addition, GaN band edge emissions at 357.8 nm and yellow band are also observed. Thus, it is likely that, for 0.5 ML nominal thickness, the QWs are sheet-like with a large lateral size variation.

6. InN OW formation mechanism

We propose a growth mechanism that can quantitatively explain the formation of the ultra-thin nominal InN QWs. As is shown in Fig. 1, after the deposition of a nominal InN QW, a Ga-rich growth condition is used to cap the QW with a pure GaN spacer. Thus, the fact that a certain amount of indium was preserved during the first one or two monolayers seems to be contradictory to the widely accepted knowledge that the Ga-rich growth condition, i.e., Ga/N flux ratio larger than unity, completely prevents indium incorporation. Therefore, it can be speculated that the Ga-rich growth condition is momentarily invalid at the beginning of GaN spacer growth stage.

A simple growth scenario, as is shown in Fig. 8, is used to demonstrate the essential features of the proposed mechanism for QW formation. The growth starts from a GaN surface covered by a single indium adlayer under active nitrogen impingement. Since InN film growth is prohibited at 550 °C due to the severe thermal decomposition, this 1-ML-thick indium adlayer remains in a liquid-like form prior to the GaN capping. On the other hand, given the fact that the growth of bulk InGaN is possible at 550 °C, the film growth must be triggered by the introduction of gallium into the 1-ML indium. Once the gallium shutter is open (step 1), newly arrived gallium adatoms start to build the second metal adlayer. At the same time, similar to what is observed in metal modulation epitaxy (MME) InGaN growth [37], an exchange process occurs such that the gallium atoms start to replace the indium atoms in the bottom adlayer (step 2), and the (InGaN) film growth is triggered. Therefore, the effective gallium flux, i.e., the rate that gallium atoms enter the growth front (the bottom metal adlayer), is very small in the beginning of GaN capping. As a result, the Ga-rich growth is not established at the beginning of the GaN capping and the incorporation of indium atoms is possible.

As the growth continues, the exchange process keeps reducing the indium concentration in the bottom adlayer (step 3) until it is fully solidified into an InGaN film (step 4). It should be pointed out that indium atoms in the InGaN film are still allowed to be replaced by the gallium atoms from the top liquid-like adlayers and, thus, the indium content in the InGaN film is further reduced. This second exchange mechanism is driven by the large difference between the InNN and GaNN binding

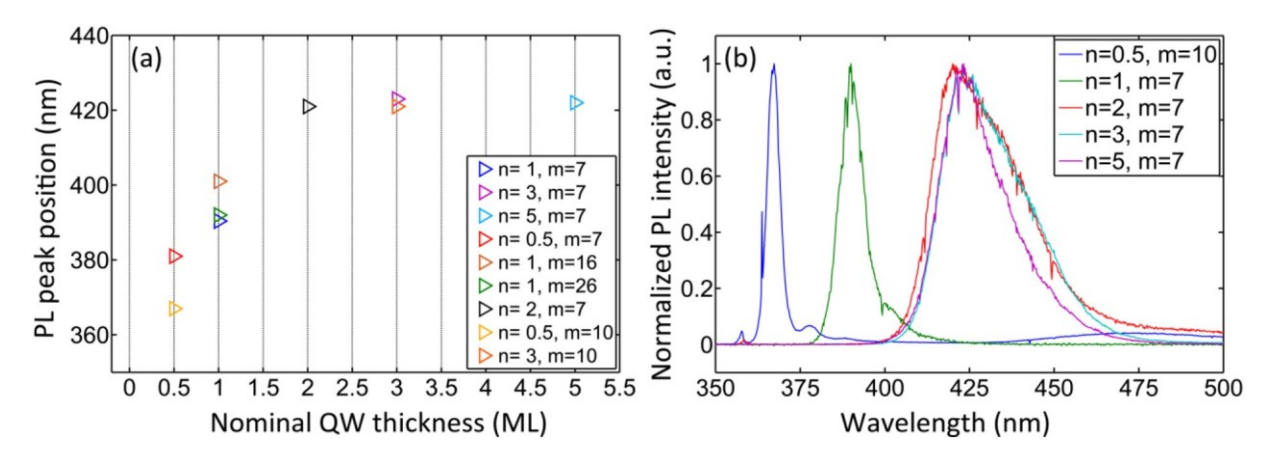


Fig. 7. (a) Summary of PL emission peaks of MQWs with different conbinations of nominal InN thickness (n) and number of QWs (m); (b) Representive PL curves for samples with various nominal thickness (n).

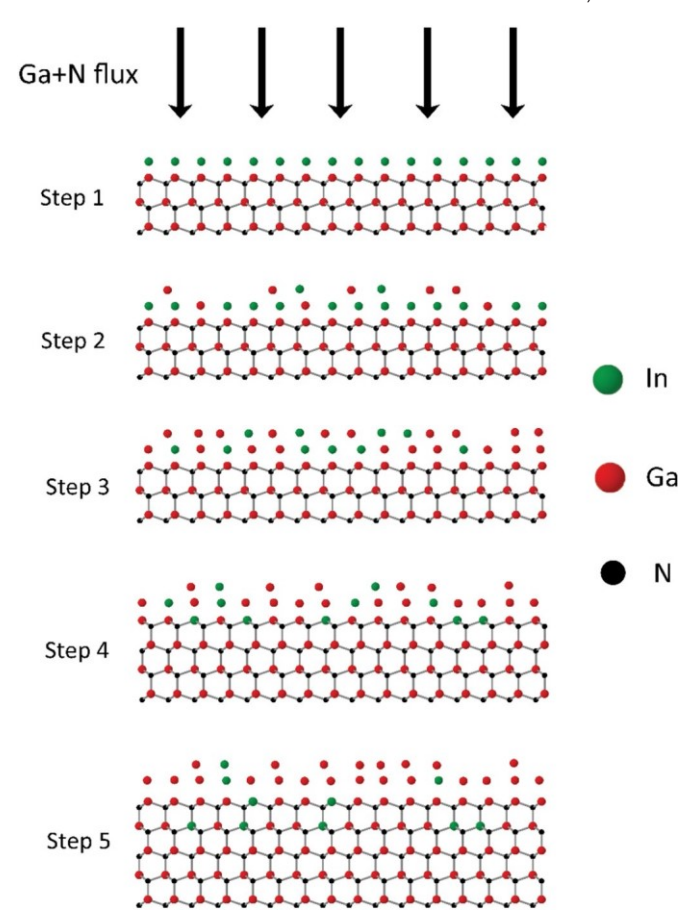


Fig. 8. Schematic illustration of the In(Ga)N QW formation process.

energies and is similar to what is observed in the study of AlN/GaN MQWs growth [38]. The knowledge of the exact indium concentration in this InGaN film requires detailed kinetic information of the exchange mechanisms and film growth. However, it is reasonable to expect that

this film is Ga-rich since the In N bonding is extremely unstable at the growth temperature of 550 °C.

Step 4 can be viewed as the initial condition for the growth of the second InGaN layer. The growth process is similar to that of the first InGaN layer except that the surface before growth is covered by Gacontaining adlayers instead of a pure indium adlayer (see step 1). Thus, it can be expected that the final indium content in the second InGaN layer is much smaller than that of the first InGaN layer (step 5). Moreover, as the GaN capping proceeds, the adlayer on the surface becomes more and more Garich and eventually the Garich growth condition is reached, and the indium incorporation becomes completely impossible.

Variations to the growth model depicted in Fig. 8 can be used to explain other growth scenarios. First of all, if in step 1 the surface is covered by two MLs of indium before growth, it can be expected that both the first and second InGaN layers are more indium-rich than the case depicted in Fig. 8, since the gallium atoms have to go through an additional indium adlayer to reach the growth front. This may explain the redshift of PL emission in Fig. 7(a) when the nominal InN QW thickness became larger. Moreover, if the surface indium coverage is further increased, excess indium other than the 2-ML adlayers will grow into droplets instead of building adlayers and a major portion of surface remains to be covered by 2-ML indium adlayers. This practically gives the same initial growth condition as the case with exactly 2-ML indium coverage and may explain the self-limited red-shifting of PL energy as well as the QW thickness.

Further, the kinetic nature of the growth model in Fig. 8 suggests non-abrupt upper interfaces of the QWs. Also, indicated by the "1+1/7" RHEED pattern prior to the nominal InN QW growth, the QW growth starts from an InGaN surface instead of a pure GaN surface except the first growth cycle, which extends the indium profile below the QWs. The widening of QW may be supported by the possible indium enrichment in the abutting monolayers of QWs observed in the recent TEM study [23].

7. Discussion and conclusions

The PAMBE growth of InN/GaN MQWs were systematically studied at the low growth temperature of 550 °C. As revealed by RHEED intensity and pattern transitions, the non-incorporated indium during the InN QW growth leads to a surface indium accumulation even for samples with InN deposition as small as 0.5 ML. Moreover, the appearance of the 1 + 1/7 RHEED pattern indicates that the indium surface accumulation produced an InGaN film at the end of GaN spacer growth. Nevertheless, the successful insertion of In(Ga)N QWs in a GaN matrix was confirmed by XRD and TEM measurements. Thus, these results explicitly show that: (i) even at low growth temperature (in our case 550 °C) not all supplied indium is incorporated into the QW (even if the nominal thickness of InN is b1 ML); and (ii) residual indium can lead to the enrichment in indium of abutting MLs on either side of QW. The last correlates with experimentally observed two additional MLs of lower indium concentration on either side of the higher indium ones for In(Ga)N/GaN multi-quantum well short period superlattices [24].

The PL emission shows a continuous redshift with the nominal InN deposition from ~370 nm for n=0.5 ML until it saturates at ~423 nm for $n\geq 2$ ML (see Fig. 7(a)). The PL emission peaks between 390 and 400 nm and at ~420 nm agree well with the reported PL data from InN/GaN QWs with 1- and 2-ML apparent thicknesses obtained under very different growth conditions [16,17]. In addition, it is shown that, when the nominal InN thickness is larger than 2 MLs, the PL emission peak positions show very small variation. A possible mechanism to explain the consistency of the PL data among different studies is that the content of the QWs is the result of the preservation of the preservation with a preservati

PR30° symmetry [15,24]. This argument is supported by the "1 × 3" RHEED pattern observed prior to the GaN spacer growth, as well as the direct TEM observation of the 3× indium atom ordering in the QW layers [24]. However, the appearance of the 1 + 1/7 pattern, caused by a incommensurate indium adlayer sitting on an InGaN surface, indicate that freezing the ${}^{p}_{3}$ ${}^{p}_{$

The study of spatial distribution of In in coherent $In_xGa_{1-x}N$ grown epitaxially on GaN(0001) using a combined method of Monte Carlo and ab initio calculations [39] provides an alternative explanation of the chemical ordering of indium atoms. It is found that low-In-content $In_xGa_{1-x}N$ epitaxial layers exhibit a strong tendency towards ordering, as highlighted by the formation of a vertical stack of the $oldsymbol{0}$ $oldsymbol{0}$ oldsym

It should be noted that pre-existing InGaN layers observed in this study, indicated by the $1\pm1/7$ RHEED pattern, would widen the indium content profile. However, the consistency of PL data suggests that the influence of this pre-existing InGaN is not large at 550 °C. This may be explained by the instability of the non-capped InGaN layers. As previously discussed, the better stability of the $1\pm1/7$ RHEED pattern under active nitrogen flux indicates that the non-capped InGaN layer is subject to decomposition through losing nitrogen atoms. This mechanism may be supported by the STM investigation of InGaN surfaces [40-42]. It was found that indium atoms in the topmost layer of an

InGaN film tend to bond to each other directly by losing the underlying nitrogen atoms when they are close to each other. Moreover, due to the well-known vertical [41–43] indium segregation, it can be expected that the InGaN layers become very indium-lean after the fairly long second growth interruption. Thus, taking into consideration the above arguments, it can be concluded that a substantial amount of indium can be frozen mainly into the first 1 or 2-MLs of In(Ga)N QW at the beginning of GaN spacer growth.

To summarize, we have studied the features of indium incorporation during the epitaxial growth of ultrathin quantum wells. Since InN film growth is prohibited at 550 °C, the In(Ga)N QW growth must be assisted by the introduction of gallium atoms. As a result, we observed an indium surface accumulation even for samples with nominal InN deposition as small as 0.5 ML. Moreover, we revealed that indium incorporates on either side of the In-rich In(Ga)N QWs. This demonstrates that ultrathin In (Ga)N QWs can survive after overgrowing with a GaN-cap layer under the Ga-rich growth conditions. At the same time, this indicates that residual surface indium results in non-abrupt In(Ga)N/GaN interfaces, which is especially influential to QWs on the order of a few monolayers thick. We assume that the growth direction profile of the In content in ultrathin In(Ga)N/GaN quantum wells depends on: (i) excess surface In from both previous InN/GaN QW growth cycles and from In overpressure for the present cycle, (ii) the growth temperature, and (iii) the strain. Finally, excess indium other than the 2-ML adlayers will grow into droplets instead of building adlayers and a major portion of the surface remains covered by 2-ML indium adlayers. This explains the selflimited epitaxial growth of ultrathin (1- to 2-ML) In(Ga)N/GaN QWs.

CRediT authorship contribution statement

Chen Li: Investigation, Formal analysis, Writing - original draft. Yurii Maidaniuk: Investigation. Andrian V. Kuchuk: Investigation, Writing - review & editing. Yuriy I. Mazur: Writing - review & editing. Mourad Benamara: Investigation. Morgan E. Ware: Writing - review & editing. Gregory J. Salamo: Supervision.

Declaration of competing interest

The authors declare that they have no known competing financial interests or personal relationships that could have appeared to influence the work reported in this paper.

Acknowledgments

This work was supported by the National Science Foundation Project "Quantum Interfaces of Dissimilar Materials" (Grant No. 1809054) and by the National Science Foundation Engineering Research Center for Power Optimization of Electro Thermal Systems (POETS) with cooperative agreement EEC-1449548.

References

- [1] S. Nakamura, T. Mukai, Jpn. J. Appl. Phys. 31 (1992) L1457.
- [2] S. Nakamura, T. Mukai, M. Senoh, Appl. Phys. Lett. 64 (1994) 1687.
- [3] S. Nakamura, M. Senoh, S. Nagahama, N. Iwasa, T. Yamada, T. Matsushita, H. Kiyoku, Y. Sugimoto, Jpn. J. Appl. Phys. 35 (1996) L217.
- [4] G.B. Stringfellow, J. Cryst. Growth 312 (2010) 735.
- [5] Z.H. Wu, Y. Kawai, Y.-Y. Fang, C.Q. Chen, H. Kondo, M. Hori, Y. Honda, M. Yamaguchi, H. Amano, Appl. Phys. Lett. 98 (2011) 141905.

- A. Yoshikawa, S.B. Che, W. Yamaguchi, H. Saito, X.Q. Wang, Y. Ishitani, E.S. Hwang, Appl. Phys. Lett. 90 (2007), 073101.
- [7] A. Yoshikawa, S.B. Che, N. Hashimoto, H. Saito, Y. Ishitani, X.Q. Wang, J. Vac. Sci. Technol. B Microelectron. Nanom. Struct. 26 (2008) 1551.
- [8] M. Anikeeva, M. Albrecht, F. Mahler, J.W. Tomm, L. Lymperakis, C. Chèze, R. Calarco, J. Neugebauer, T. Schulz, Sci. Rep. 9 (9047) (2019).
- [9] M. Siekacz, P. Wolny, T. Ernst, E. Grzanka, G. Staszczak, T. Suski, A. Feduniewicz-Żmuda, M. Sawicka, J. Moneta, M. Anikeeva, T. Schulz, M. Albrecht, C. Skierbiszewski, Superlattice. Microst. 133 (2019), 106209.
- [10] N. Chery, T.H. Ngo, M.P. Chauvat, B. Damilano, A. Courville, P.D. Mierry, T. Grieb, T. Mehrtens, F.F. Krause, K.M. Caspary, M. Schowalters, B. Gil, A. Rosenauer, P. Ruterana, J. Microsc. 268 (2017) 221.
- [11] C. Chèze, M. Siekacz, F. Isa, B. Jenichen, F. Feix, J. Buller, T. Schulz, M. Albrecht, C. Skierbiszewski, R. Calarco, H. Riechert, J. Appl. Phys. 120 (2016), 125307.
- [12] L. Zhou, E. Dimakis, R. Hathwar, T. Aoki, D.J. Smith, T.D. Moustakas, S.M. Goodnick, M.R. McCartney, Phys. Rev. B 88 (125310) (2013).
- [13] G. Staszczak, I. Gorczyca, T. Suski, X.Q. Wang, N.E. Christensen, A. Svane, E. Dimakis, T.D. Moustakas, J. Appl. Phys. 113 (2013), 123101.
- T.D. Moustakas, J. Appl. Phys. 113 (2013), 123101.E. Dimakis, A.Y. Nikiforov, C. Thomidis, L. Zhou, D.J. Smith, J. Abell, C.-K. Kao, T.D
- Moustakas, Phys. Status Solidi 205 (2008) 1070.
 [15] C. Chèze, F. Feix, M. Anikeeva, T. Schulz, M. Albrecht, H. Riechert, O. Brandt, R. Calarco, Appl. Phys. Lett. 110 (2017), 072104.
- [16] A. Yoshikawa, K. Kusakabe, N. Hashimoto, E.-S. Hwang, D. Imai, T. Itoi, J. Appl. Phys. 120 (2016) 225303.
- [17] A. Yoshikawa, K. Kusakabe, N. Hashimoto, D. Imai, E.-S. Hwang, J. Appl. Phys. 120 (2016) 235302.
- [18] P. Wolny, M. Anikeeva, M. Sawicka, T. Schulz, T. Markurt, M. Albrecht, M. Siekacz, C. Skierbiszewski, J. Appl. Phys. 124 (2018), 065701.
- [19] M.S. Miao, Q.M. Yan, C.G. Van de Walle, Appl. Phys. Lett. 102 (2013) 102103.
- [20] I. Gorczyca, T. Suski, N.E. Christensen, A. Svane, J. Phys. Condens. Matter 30 (2018), 063001.
- [21] I. Gorczyca, T. Suski, P. Strak, G. Staszczak, N.E. Christensen, Sci. Rep. 7 (2017), 16055.
- [22] T. Suski, T. Schulz, M. Albrecht, X.Q. Wang, I. Gorczyca, K. Skrobas, N.E. Christensen, A. Svane, Appl. Phys. Lett. 104 (2014), 182103.
- [23] G.P. Dimitrakopulos, I.G. Vasileiadis, C. Bazioti, J. Smalc-Koziorowska, S. Kret, E. Dimakis, N. Florini, T. Kehagias, T. Suski, T. Karakostas, T.D. Moustakas, P. Komninou, J. Appl. Phys. 123 (2018), 024304.
- [24] L. Lymperakis, T. Schulz, C. Freysoldt, M. Anikeeva, Z. Chen, X. Zheng, B. Shen, C. Chèze, M. Siekacz, X.Q. Wang, M. Albrecht, J. Neugebauer, Phys. Rev. Mater. 2 (2018), 011601.
- [25] C. Adelmann, R. Langer, G. Feuillet, B. Daudin, Appl. Phys. Lett. 75 (1999) 3518.
- [26] M. Moseley, D. Billingsley, W. Henderson, E. Trybus, W.A. Doolittle, J. Appl. Phys. 106 (2009), 014905.
- [27] C. Li, Y. Maidaniuk, A.V. Kuchuk, S. Shetty, P. Ghosh, T.P. White, T.A. Morgan, X. Hu, Y. Wu, M.E. Ware, Y.I. Mazur, G.J. Salamo, J. Appl. Phys. 123 (2018) 195302.
- [28] I.-S. Shin, K. Wang, T. Araki, E. Yoon, Y. Nanishi, Appl. Phys. Express 5 (2012), 125503.
- [29] T. Araki, H. Umeda, T. Yamaguchi, T. Sakamoto, E. Yoon, Y. Nanishi, 2010 22nd Int. Conf. Indium Phosphide Relat. Mater, IEEE, 2010 1–4.
- [30] A.R. Smith, J. Vac. Sci. Technol. B Microelectron. Nanom. Struct. 16 (1998) 2242.
- [31] M. Ritter, W. Ranke, W. Weiss, Phys. Rev. B 57 (1998) 7240
- [32] H. Zi-Pu, D.F. Ogletree, M.A. Van Hove, G.A. Somorjai, Surf. Sci. 180 (1987) 433.
- [33] C. Friedrich, A. Biermann, V. Hoffmann, M. Kneissl, N. Esser, P. Vogt, J. Appl. Phys. 112 (2012), 033509.
- [34] K. Kusakabe, N. Hashimoto, T. Itoi, K. Wang, D. Imai, A. Yoshikawa, Appl. Phys. Lett. 108 (2016), 152107.
- [35] T. Yamaguchi, N. Uematsu, T. Araki, T. Honda, E. Yoon, Y. Nanishi, J. Cryst. Growth 377 (2013) 123.
- [36] Di. Ma, X. Rong, X. Zheng, W. Wang, P. Wang, T. Schulz, M. Albrecht, S. Metzner, M. Müller, O. August, F. Bertram, J. Christen, P. Jin, M. Li, J. Zhang, X. Yang, F. Xu, Z. Qin, W. Ge, B. Shen, X. Wang, Sci. Rep. 7 (2017) 46420.
- [37] M. Moseley, B. Gunning, J. Greenlee, J. Lowder, G. Namkoong, W. Alan Doolittle, J. Appl. Phys. 112 (2012), 014909.
- [38] A.V. Kuchuk, V.P. Kladko, T.L. Petrenko, V.P. Bryksa, A.E. Belyaev, Y.I. Mazur, M.E. Ware, E.A. DeCuir, G.J. Salamo, Nanotechnology 25 (2014), 245602.
- [39] S. Lee, C. Freysoldt, J. Neugebauer, Phys. Rev. B 90 (2014), 245301.
- [40] H. Chen, R.M. Feenstra, J.E. Northrup, T. Zywietz, J. Neugebauer, Phys. Rev. Lett. 85 (2000) 1902.
- [41] H. Chen, R.M. Feenstra, J.E. Northrup, T. Zywietz, J. Neugebauer, D.W. Greve, J. Vac. Sci. Technol. B Microelectron. Nanom. Struct. 18 (2000) 2284.
- [42] H. Chen, R.M. Feenstra, J.E. Northrup, J. Neugebauer, D.W. Greve, MRS Internet J. Nitride Semicond. Res. 6 (2001) e11.
- [43] S.Y. Karpov, Y.N. Makarov, Phys. Status Solidi 188 (2001) 611.